

Microstructural and Mechanical Characterization of Friction Stir Processed Aluminum Alloy 6061-T6 Reinforced with Zirconium-Silicate Particles

Zohreh Ebrahimi^{1*}, Moslem Sarikhani¹

¹Mechanical Engineering Department, Payame Noor University (PNU), P.O.Box 19395-4697 Tehran, Iran

*Email of the Corresponding Author: z.ebrahimi@pnu.ac.ir

Received: September 2, 2023; Accepted: November 11, 2023

Abstract

Friction stir processing (FSP) is an effective technique for surface modification and grain refinement. This method can be used to incorporate hard ceramic reinforcement into modified aluminum surfaces, allowing for the fabrication of composites with enhanced properties. In this study, FSP was utilized to fabricate surface composites of aluminum alloy 6061-T6 reinforced with zirconium-silicate particles. The effects of tool rotational and traverse speeds, as well as the number of passes, on the microstructural and mechanical properties of the composite specimens were investigated. The corresponding strength, grain size, and microhardness of the specimens were evaluated and compared with unprocessed and non-reinforced aluminum alloy. The scanning electron micrographs of the specimen cross-section showed an excellent dispersion of zirconium-silicate particles in the aluminum matrix, indicating the homogeneity of the aluminum composite and the success of the applied FSP. The results showed that increasing the number of passes from one to four caused microstructure refinement at the stir zone, resulting in enhanced tensile strength and hardness of the produced composite. An optimum value of 1000 rpm and 20 mm/min for rotational and traverse speeds was obtained. Consequently, a composite with improved mechanical properties was achieved due to the formation and distribution of reinforcing zirconium-silicate particles.

Keywords

Friction Stir Process, Reinforcing Particles, AL6061-T6/ZrSiO₄ Composite, Microhardness

1. Introduction

In the FSP method a frictional heat and stirring action lead to microstructural modification, dynamic recrystallization, and significant refinement in the nugget zone [1]. The frictional heat is caused by the high-speed rotation of a cylindrical tool with a pin and shoulder that traverse forward. The FSP involves severe plastic deformation and temperature increasing due to the frictional heating in the near-surface layers of the metallic material. FSP also offers possibility of particle reinforcement incorporation in the nugget zone to make a surface composite and creates a fine and equiaxed microstructure. The FSP process parameters affect microstructure, mechanical properties and the distribution of the reinforcing particles. Kwon and Saito [2] have reported improvement of hardness and tensile strength of the friction stir processed (FSPed) 1050 aluminum alloy with decreasing of the tool rotational speed. Nakata et al. [3] have used a multi-pass FSP to enhance the mechanical

properties of an aluminum die casting alloy. Su et al. [4] have produced very fine grains in a commercial 7075 aluminum alloy by a cooling rate-controlled FSP method. The effects of the friction stir welding tool pin and rotational speed on the mechanical properties of the AA6061 aluminum alloy has been studied by Elangovan and Valliappan [5]. They found that the joints fabricated using the tool with square pin and rotational speed of 1200 rpm exhibited the more enhanced tensile strength and hardness. Karthikeyan et al. [6] have studied the microstructural properties of the FSPed cast aluminum 2285 alloy under different rotational and traverse speeds of the tool pin and obtained optimum FSP parameters to enhance strength and ductility of the processed material. Morishige et al. [7] have treated the microstructure refinement in pure aluminum using the FSP method. They have reported a minimum grain size at high strain rates of the FSP process. In another study, the mechanical properties of multi-pass FSPed aluminum 6063 have been investigated with different overlapping percentage [8]. This research revealed the negative effect of the overlapping percentage on the strength and hardness of the FSPed specimens due to the dissolution of the hardening precipitates. Devaraju et al. [9] have fabricated and tested aluminum alloy surface composites by incorporating Silicon carbide (SiC) reinforcing particles via FSP. Their examinations indicated that the reinforcing SiC particles are uniformly dispersed in the nugget zone. The effects of FSP parameters on the microstructural and mechanical properties of aluminum 6082 is addressed by El-Rayes and El-Danaf [10]. They observed an increase in the FSP dynamic recrystallization of the stir zone with increasing the number of passes which leads to equiaxed grains with high angle grain boundaries. The corrosion resistance of an FSPed AA5083 aluminum alloy has been studied by Rasouli et al. [11]. They found that the FSPed specimens exhibited higher corrosion resistance compared with the base metal. Alishavandi et al. [12] have applied FSP on AA1050 aluminum alloy and reported improved hardness and tensile strength of the FSPed samples. Valeeva et al. [13] have studied the effect of the tool pin length on the strength of the 2024 aluminum alloy processed with the FSP method. They obtained a necessary and sufficient pin length that provides mixing throughout the thickness of the specimen. Mirian Mehrian et al. [14] have investigated the effects of FSP parameters, such as the tool rotational and traverse speeds, on the microstructural and mechanical properties of Al-Mg alloys. Their investigations revealed significant grain refinement in the FSPed Al-Mg alloy.

Improving the material properties using the nanoparticles as reinforcement has attracted the attention of many researchers recently [15-16]. The creation of a composite layer on the surface of metals and alloys is a major application of the friction stir process. Producing a surface FSP composite on the alloy substrate causes the excellent surface properties of the composites while maintaining the overall mechanical properties of the base metal. Utilizing the FSP process has increased the application of aluminum and its alloys in the aerospace, automotive, transportation, marine, structural construction, and electrical industries. Soleymani et al. [17] have investigated the microstructural properties of the FSPed AL5083 surface hybrid composite and reported a uniform distribution of reinforcing particles inside the stir zone. Kumar et al. [18] have reviewed current studies regarding the effect of the FSP process on the microstructure and mechanical properties of aluminum alloys and their composites. Moustafa et al. [19] have applied the FSP process to fabricate a surface composite layer of AL2024 alloy reinforced with various nanoparticles. They incorporated reinforcement particles into double and triple hybrid composites and determined the most effective combination for a significant improvement in the hardness and wear properties. Liu et al. [20] have fabricated novel graphene-

aluminum composites by the FSP process. They observed a large number of graphene-aluminum nano-clusters embedded in the grain interior of the aluminum matrix with a semi-coherent bond between graphene and aluminum. Huang et al. [21] have produced and characterized particle-reinforced aluminum matrix composites using FSP. They found that increasing the volume fraction of tungsten carbide particles enhances the strength and hardness but decreases the ductility of the processed materials. In another study, the AA6061-Al₃Fe cast aluminum matrix composites were prepared by adding iron particles to an aluminum matrix using the FSP process [22], where a homogeneous distribution of the iron particles in the produced composite is found. Madhu et al. [23] have developed an AL-TiO₂ nanocomposite using the FSP process. Their results revealed that the particle refinement and dispersion lead to a homogeneous matrix with higher mechanical properties. Many surface composites have been fabricated by FSP incorporating SiC particles [24]. Asadi et al. [25] have used FSP to produce SiC/AZ91 composite layers at different process parameters. They found that FSP is an effective method to fabricate sufficiently refined and uniform composite layers. Dolatkhah et al. [26] have investigated the microstructure and mechanical properties of FSPed AA5052 aluminum alloy reinforced with SiC particles. They found optimum values of the tool rotational and traverse speed and SiC particle size to achieve the desired wear resistance and hardness of the FSPed specimens. Zuhailawati et al. [27] have developed a surface composite using FSP of AA6061-T6 aluminum alloy reinforced with amorphous silica. The hard silica particles restricted the grain growth of the aluminum matrix and caused a slight increase in the hardness of the produced composite. Sharma et al. [28] have produced defect-free metal matrix composites and improved the wear resistance of the 7075 aluminum alloy reinforced with boron carbide particles using friction stir processing. Khethier Abbass and Baheer [29] found that the addition of SiC particles to AA6061-T6 improves the hardness and wear properties of the fabricated surface composites as compared to the processed specimens without reinforcing SiC particles. Dwivedi et al. [30] have produced the surface AA5083 composite via the FSP process using a mixture of SiC and other metal powder. They performed microstructural characterization to study various zones of the FSPed specimens and observed that grain size varies from one zone to another and enhances the mechanical properties of the FSPed samples. Subramani et al. [31] have used the FSP process to make a hybrid composite from AA6061 reinforced with B₄C and SiC particles. They have observed a uniform distribution of SiC-B₄C elements in the FSPed AA6061 matrix. Ande et al. [32] have applied the FSP process to produce 7075-T651 aluminum alloy surface composites with SiC particles as reinforcement. They found that the average hardness of the stir zone of composite samples is higher than that of the base metal. Ceramic particles with good hardness and wear resistance are considered potential reinforcements which include carbide (SiC), alumina, boron carbide (B₄C), graphite, quartz, and zirconium silicate (ZrSiO₄) [33]. Among these, zirconium silicate is a very promising reinforcement in light metals especially where improved mechanical and wear properties are required [34]. Also, zirconium silicate is known to exhibit high hardness, strength, density, fracture toughness, chemical inertness, and wear resistance with a low coefficient of thermal expansion which makes it suitable for enhancing aluminum alloy properties in automobile industries and construction applications [35]. A review of the effect of ZrSiO₄ on the mechanical properties of aluminum composites is reported which indicates that ZrSiO₄ can be applied to improve the ultimate tensile strength and hardness of aluminum alloys [36]. Aluminum A356/ZrSiO₄ metal matrix composite has been fabricated by Kumar et al. [37] by

using the stir casting method. They concluded that the reinforcement addition improves the wear resistance of the composite and is suitable for cylinder blocks in automobiles. The addition of ZrSiO₄ improves the bonding strength of the matrix-reinforcement interface, which enhances the composite hardness [38]. Moreover, the test samples T6 heat treatment carried out by Fabrizi et al. [39] have significantly affected the composite. Dhuruva Maharishi et al. [40] prepared aluminum 365 alloy metal matrix composite by stir casting method at four different weight fractions of the ZrSiO₄ reinforcement particles. They found an optimum value of 5 percent of particle weight fraction and observed a ductile fracture mode in the composites having 3 and 5 wt% ZrSiO₄ ceramic particles. Most of the mentioned literature has considered silicon or boron carbide as reinforcement to produce FSPed aluminum surface composites. Rahsepar and Jarahimoghdam [41] have used ZrSiO₄ particles to produce aluminum AA5052 surface composite using the FSP process. They investigated the mechanical and corrosion behavior of the FSPed composites for different friction stir pass numbers. They enhanced the composite performance by increasing the number of the FSP passes to three. To the best of the author's knowledge, the FSP process of aluminum AL6061 alloys to produce surface composites using reinforcing zirconium-silicate particles has not been reported in the literature. Aluminum AL6061-T6 is used widely in the automotive, aerospace, and food industries due to its high strength-to-weight ratio and good fatigue resistance. The wing and fuselage of small aircraft, wheel spacer of automobiles, and packing cans of food-stuffs are made of AL 6061 alloy. In this research, the FSP process of aluminum alloy 6061-T6 (AL6061-T6) is performed using zirconium-silicate particles as reinforcement. The ZrSiO₄ reinforcing particles are used to create the surface composite layer. A complete parameter study has been performed to investigate the microstructure and mechanical properties of the resulting composites. The effects of process parameters, such as tool rotational and traverse speeds, tool pin type, and the number of welding passes, on the strength and hardness of the AL6061-T6 alloy, are determined. The grain size, microhardness, and tensile strength of the produced composite layer are obtained for different process parameters.

2. Materials and Methods

The base material in this study is aluminum alloy 6061-T6 with a thickness of 5 mm. The chemical composition of the base material is reported in Table 1. The samples are cut with dimensions of 142×42 mm. The ZrSiO₄ powder is filled into a groove of 1×2 mm created in the center of the specimens in the longitudinal direction, as shown in Figure 1. Before the FSP process, the specimens are cleaned and placed in the milling machine fixture.

Table 1. Chemical composition of the AL6061-T6 plate (weight percent %)

Al	Fe	Mg	Cr	Cu	Zn	Ti	Si
Base	0.26	0.88	0.16	0.23	0.03	0.01	0.69
Mn	Ni	V	Zr	Sb	Pb	Be	pb
0.0248	0.005	0.02	Trace	0.0018	0.0011	Trace	0.003

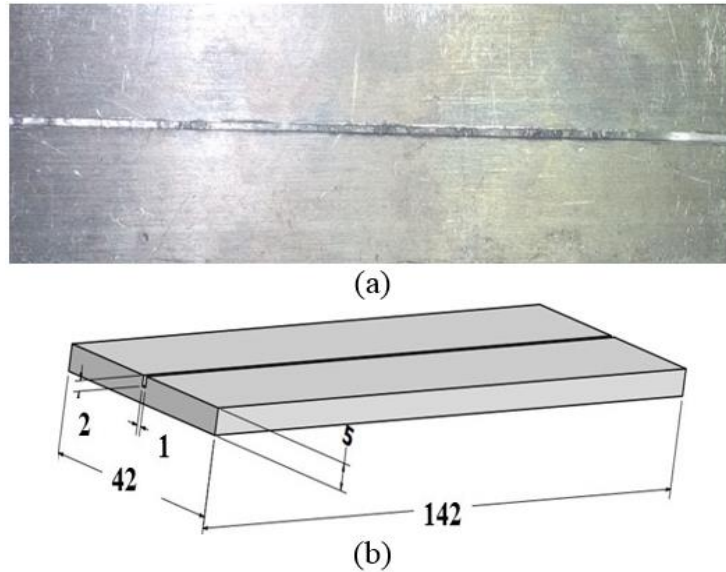


Figure 1. Aluminum plate and the groove on its surface a) AL6061 plate, b) schematic of the plate and the groove (all dimensions are in mm)

The zirconium-silicate powder with an average size of $5\ \mu\text{m}$ and one gram per specimen is used as reinforcing particles. The threaded cylindrical pins are the most suitable tools for the FSP process of aluminum alloys. First, a no-pin tool is used to trap zirconium-silicate particles inside the groove (Figure 2a) and then a tool with a simple shoulder and a threaded pin is used to perform the FSP process (Figure 2b). The H13 steel tools are used in this study, and their dimensions are shown in Figure 2c. The tool rotational speed (V_{RS}) and traverse speed (V_{TS}) are changed from 800 to 1600 rpm and 16 to 63 mm/min, respectively. The tilt angle is 3° and a penetration depth of 1 mm is applied. The specimen after the FSP process is shown in Figure 2d. Different numbers of passes are used to prepare the FSPed samples. A complete parameter study is carried out by applying different pass numbers and traverse and rotational speeds.

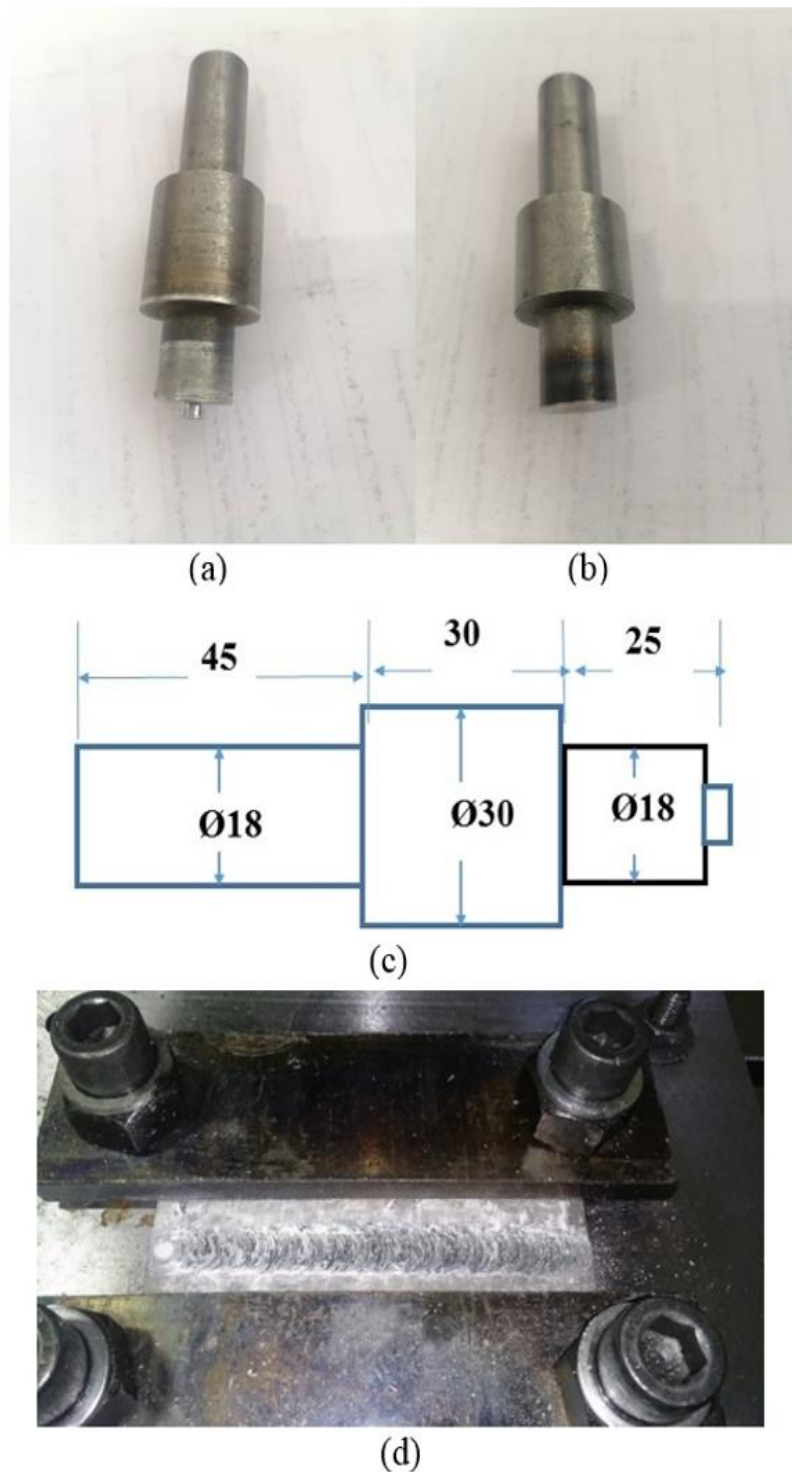


Figure 2. a) No-pin tool, b) tool with a threaded pin used for the FSP, c) schematic of the FSP tool (all dimensions are in mm) d) the specimen after the FSP process

After the FSP process, the specimens are cut in the traverse direction for microstructural studies. The composite surfaces of the FSPed specimens are prepared by standard polishing and etching techniques according to mechanical grinding on SiC emery papers up to grade #2522. This procedure is followed by polishing with 2.3 μm alumina powder. The material structure is etched with a solution containing 50 ml Poulton's chemical reagent, 5 gr NaF, and 2 gr NaOH. Then, the resulting composite

microstructure and the distribution of the ZrSiO₄ particles in the stirred zone are investigated by optical microscopy.

Vickers hardness tester with a load of 52 g at a distance of 1.5 mm from the upper surface of the rectangular samples has been used to evaluate the microhardness of the FSPed specimens. The microhardness tests are performed on longitudinal lines at 0.5 mm consecutive points. The KOOPA hardness tester is used for microhardness evaluations.

Next, the tensile tests are carried out according to ASTM E8/E8M-09 standard using a STMSANTAM-250 machine at a strain rate of 10^{-3} s^{-1} . Tensile samples are machined from the surface of the composite normal to the FSP direction, using a wire electric discharge machine, and the schematics of dimensions and the specimens after the tensile tests are shown in Figure 3.

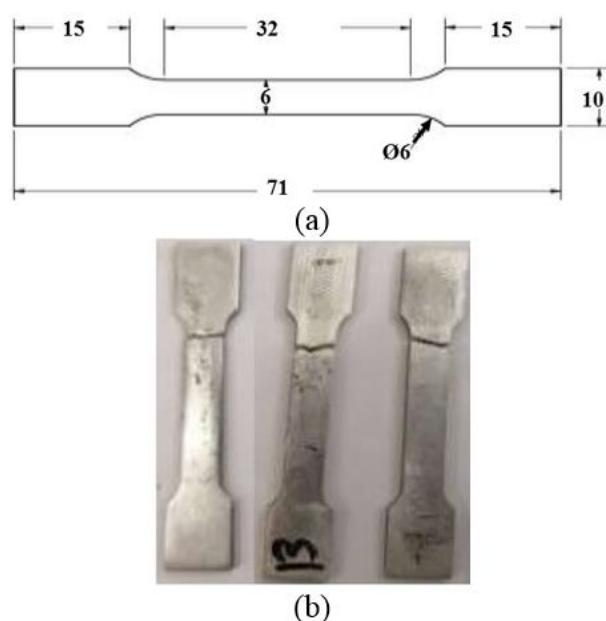


Figure 3. a) Schematic of the tensile test specimen (all dimensions are in mm), b) the fractured samples after the tensile tests

The dispersion of the zirconium-silicate particles is observed by the scanning electron microscope (SEM) at a fractured cross-section of a tensile test specimen with four passes, $V_{ST} = 20 \text{ mm/min}$ and $V_{RS} = 1000 \text{ rpm}$. A model of the TESCAN-Vega3 scanning electron microscope manufactured by TESCAN Company (Czech Republic) placed at the central laboratory of Shiraz University is used. The specimen for the observation is cut from the central part of the tensile test specimen. The surface of the specimen was cleaned and polished with alumina powder and was slightly coated with gold for the SEM observation.

3. Results and Discussion

First, the microstructure of the FSPed aluminum alloy reinforced with zirconium-silicate particles is investigated. Figure 4 shows the SEM images of the tensile test specimen with four passes, $V_{TS} = 20 \text{ mm/min}$ and $V_{RS} = 1000 \text{ rpm}$. The fractured cross-section of the specimen exhibits excellent dispersion of the ZrSiO₄ particles.

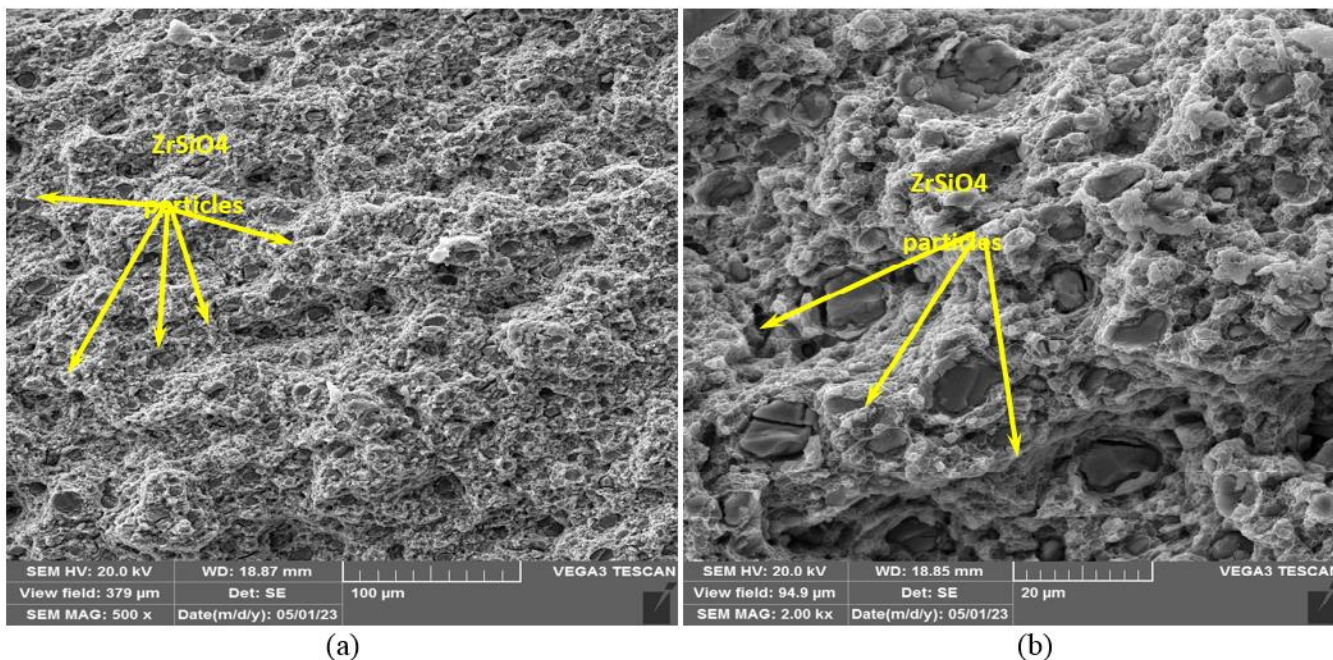


Figure 4. SEM image of the fracture surface of the tensile test specimen at magnifications of a) 500X and b) 2000X

The boundary between the base metal and the stir zone (SZ) is distinguished in Figure 5, where the FSP process has led to grain refinement in the SZ. The grain refinement in the stir zone can be attributed to large strains, the resulting dynamic recrystallization, and the pinning effects of the ZrSiO₄ particles. On the other hand, using zirconium-silicate particles with a very low thermal conductivity causes an increase in temperature in the region and an annealing effect, which increases the grain size. However, the grain refinement is controlled more by the pinning effects of the ZrSiO₄ particles.

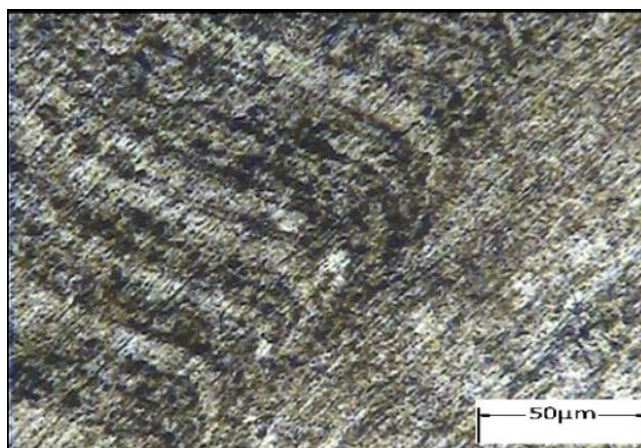


Figure 5. The stir zone microstructure of the FSPed AL6061-T6/ ZrSiO₄

Next, the effects of the FSP parameters on the grain size of the AL60601/ZrSiO₄ composite are investigated. Figure 6 shows the SZ microstructure of the FSPed specimens with four passes, $V_{TS} = 20$ mm/min, and different tool rotational speeds, i.e. $V_{RS} = 800, 1000, 1250,$ and 1600 rpm. It can be seen that with increasing V_{RS} , the average grain size has increased. The dynamic recrystallization increases with tool rotational speed, due to

the increase in tool stir effects and material flow. On the other hand, the inlet temperature of the specimen increases with increasing the tool stirring effect. Hence, the effect of the annealing overcomes the recrystallization effects, and the grain size increases. The FSPed specimen with four passes, $V_{TS} = 20$ mm/min and $V_{RS} = 1000$ rpm has the grain size of about $3 \mu\text{m}$ and increases to $5 \mu\text{m}$ by increasing V_{RS} to 1600 rpm. However, further SEM investigations are required for a more accurate evaluation of the grain size, which is beyond the scope of the present study.

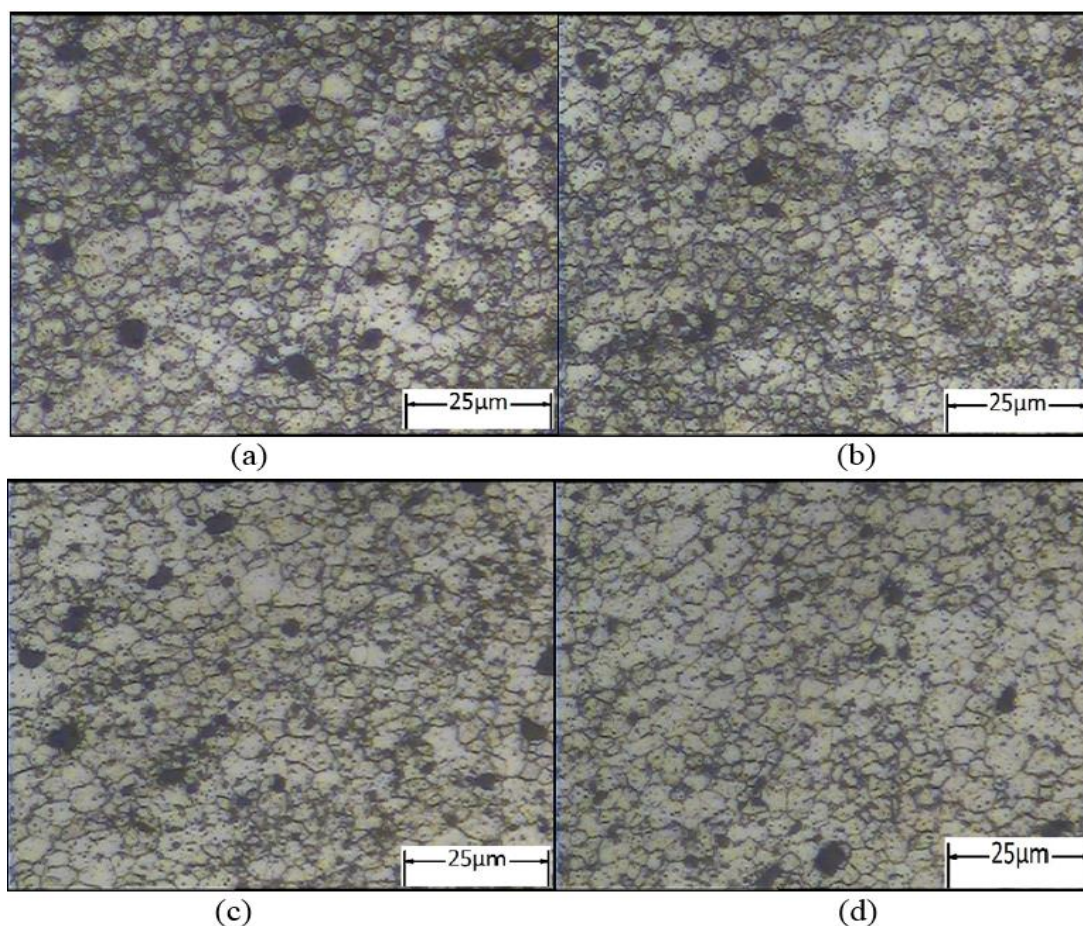


Figure 6: The microstructure of the stir zone of the FSPed samples with different FSP tool rotational speeds, a) 800, b)1000, c) 1250, d) 1600 rpm

Figure 7 shows the SZ microstructure of the FSPed composite specimens with four passes, $V_{RS} = 1000$ rpm, and different traverse speeds, i.e. $V_{TS} = 16, 20, 40,$ and 63 mm/min. The smallest grain size (about $3 \mu\text{m}$) is obtained for $V_{TS} = 20$ mm/min as shown in Figure 7b. In Figures 7c and 7d, the grain size has increased to about $6 \mu\text{m}$. In Figure 7a, which has the lowest traverse speed ($V_{TS} = 16$ mm/min) and the highest heat generation, the phenomenon of dynamic recrystallization and grain growth has occurred. In other words, small grains were initially created, but these grains have grown larger due to the high heat and sufficient time, which was provided because of the low traverse speed. In Figure 7b, the heat has decreased slightly. Hence, only dynamic recrystallization has occurred and the grains have become smaller, but grain growth has not happened. In

Figures 7c and 7d, the heat has decreased significantly with the increase in traverse speed, and the phenomenon of dynamic recrystallization has not occurred at all or has taken place to a small extent. Hence, the grains have remained coarse, like the initial grains. Moreover, the highest tensile strength and strain, which are among the characteristics of small grains, belong to $V_{TS} = 20$ mm/min in Figure 7b. Therefore, the tensile strength, hardness, and strain will increase initially with the increase in traverse speed and then, they will decrease with a further increase in the traverse speed. The effect of V_{TS} on the mechanical properties of the FSPed samples of AL60601/ZrSiO4 composite is discussed in more detail in the continuation of the present study.

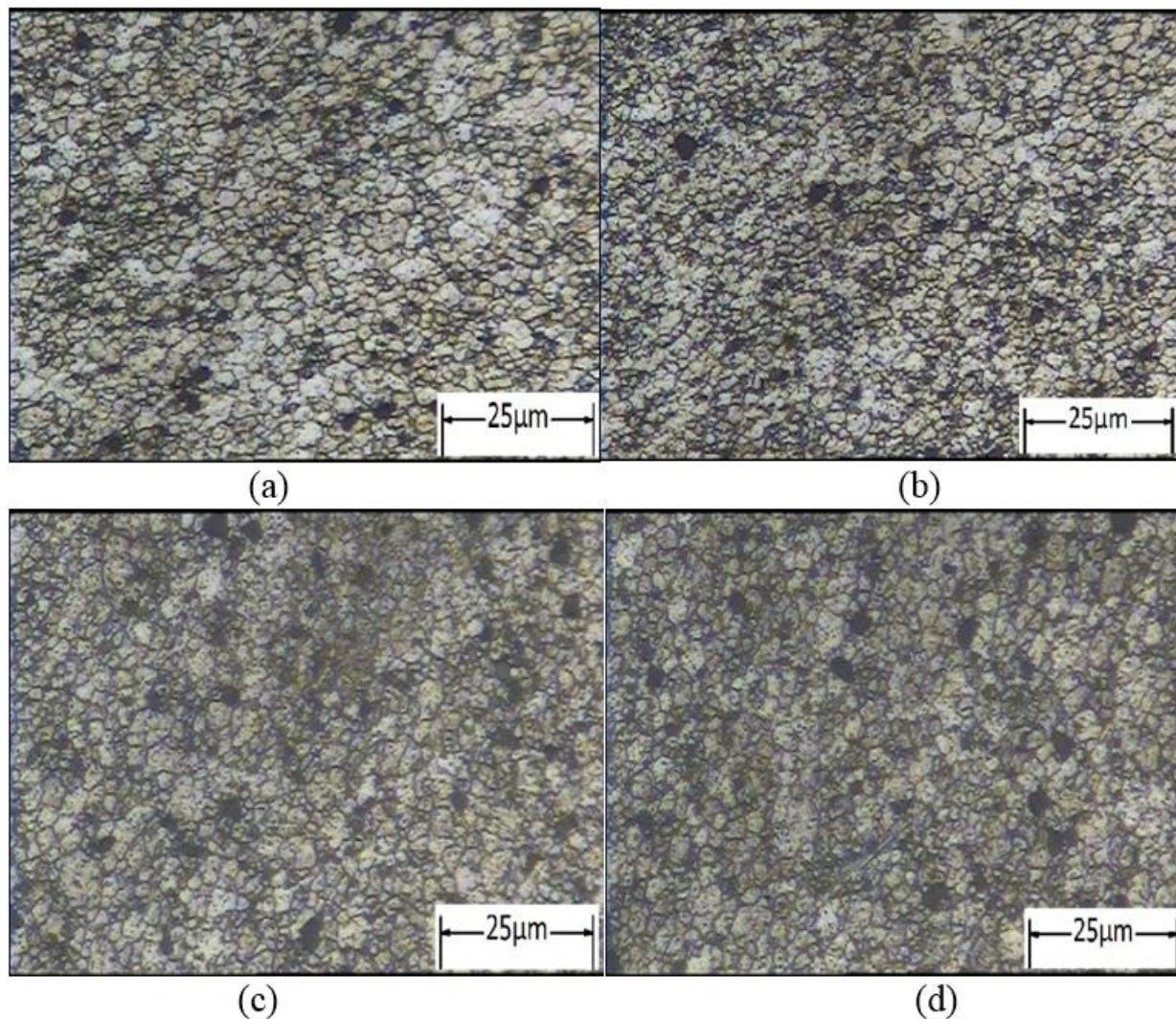


Figure 7. The microstructure of the stir zone of the FSPed samples with different FSP tool traversing speeds, a) 16 mm/min, b) 20 mm/min, c) 40 mm/min, d) 63 mm/min

The effect of pass number on the microstructure of the FSPed composite specimens has also been studied. Figure 8 shows the SZ microstructure of the FSPed AL6061-T6/ZrSiO4 composites, for 1, 2, and 4 passes with $V_{TS} = 20$ mm/min and $V_{RS} = 1000$ rpm. As can be seen, the grain size of the composite produced with four passes has decreased compared to the single pass. As the number of passes increases, the size of the zirconium-silicate particles becomes smaller due to the significant

mechanical stresses in the SZ. Hence, a severe recrystallization occurs and the grain size reduces. Moreover, increasing the pass number causes a better distribution of the ZrSiO₄ particles in the base phase, which increases the pinning effect of the zirconium-silicate particles and reduces the grain size. The grain size has decreased from approximately 8 μm to 3 μm by increasing the pass number from one to four.

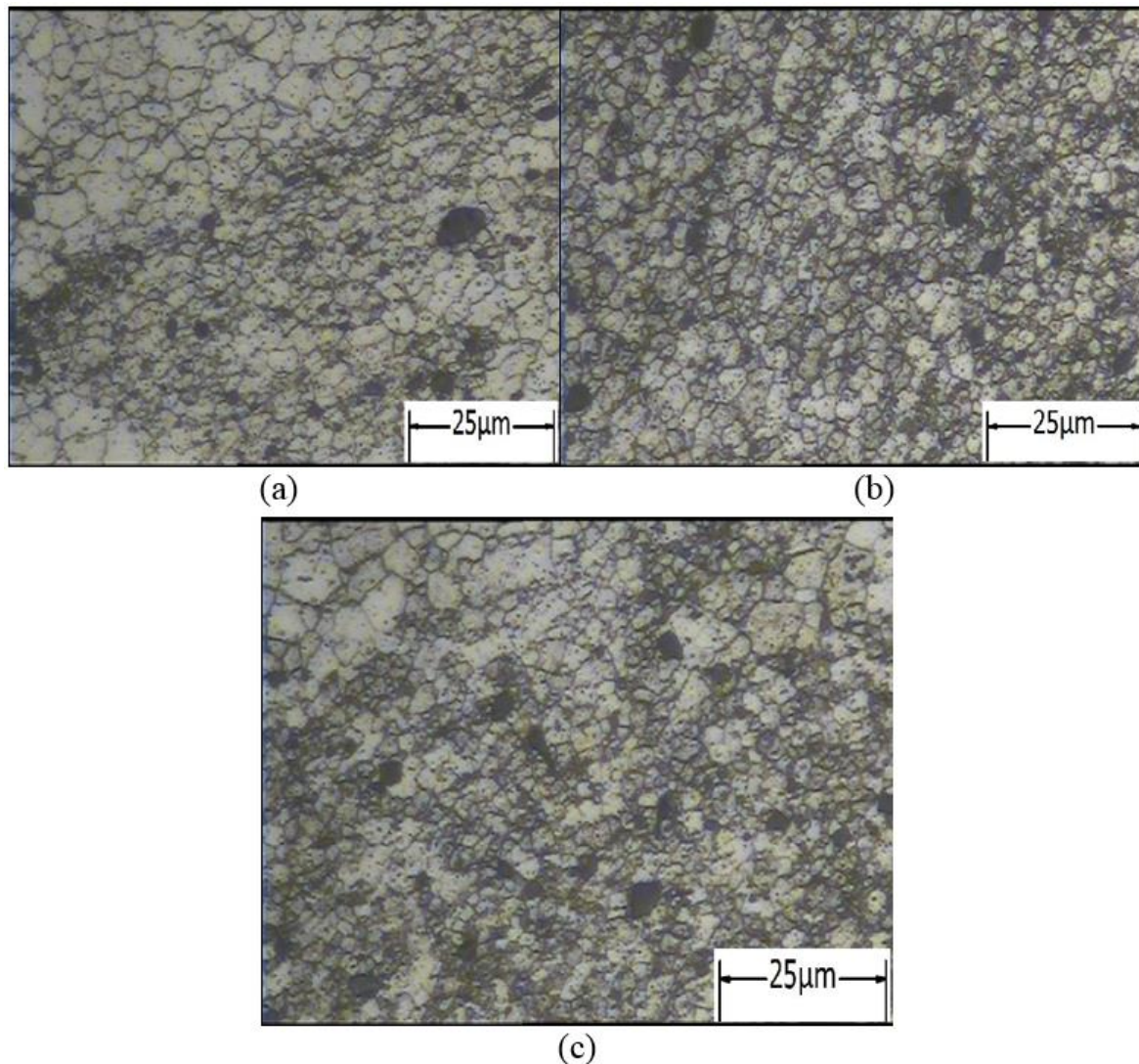


Figure 8. The microstructure of the stir zone of the FSPed samples with $V_{RS} = 1250$ rpm, $V_{TS} = 20$ mm/min, and different numbers of passes, a) 1, b) 2, and c) 4 passes

Microhardness evaluation is performed before and after the FSP process. Figure 9 shows the microhardness curve of the composite produced with $V_{RS} = 1000$ rpm, $V_{TS} = 20$ mm/min, and one pass. Comparing it with the unprocessed AL6061-T6 microhardness curve shows that the use of zirconium-silicate particles as reinforcement in the FSP process increases significantly the hardness of the AL6061-T6/ZrSiO₄ composite. Moreover, the microhardness in the SZ has increased significantly, which can be attributed to the reduction of the ZrSiO₄ particle size due to mechanical recrystallization and the high rotational speed of the FSP tool. Each particle of the base metal material is forced to rotate in a larger direction with a rotating tool and withstand more strain. Zirconium-

silicate particles have high hardness, so further mixing and homogenizing of these materials with aluminum particles will cause high hardness.

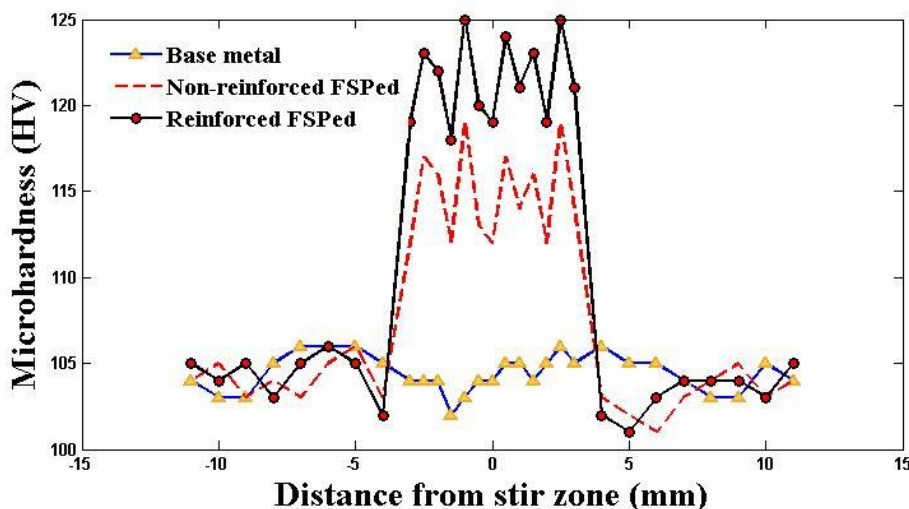


Figure 9. Microhardness of the AL6061-T6/ZrSiO₄ composite with and without FSP

Various factors control the hardness of the FSPed metal matrix composites, including mechanical recrystallization, pinning, and annealing [42]. The effects of the FSP parameters on the microhardness of the AL6061-T6/ZrSiO₄ composites were discussed in Figure 10. Figure 10a shows the microhardness curve of the composite produced with four passes, $V_{TS} = 20$ mm/min, and different V_{RS} , i.e., 1000, 1250, and 1600 rpm. At higher rotational speeds, the microhardness curves show fewer fluctuations compared to the case with lower rotational speeds, due to the better distribution of zirconium-silicate particles and production of a more homogeneous composite structure. Further reduction of the grain size and the increase in the resistance of zirconium-silicate particles against grain boundary movements, leads to an increase in the hardness of the samples. On the other hand, by increasing the tool rotational speed, the annealing effect overcomes other factors and increases the average particle size in the SZ. Therefore, the hardness decreases with increasing rotational speed. $V_{RS} = 1000$ rpm is an optimum value in this study. Figure 10b shows the microhardness changes of the FSPed composites with four passes, $V_{RS} = 1000$ rpm, and different traverse speeds of $V_{TS} = 16$, 20, 40, and 63 mm/min. As the tool advances faster, the hardness of the specimen decreases. The reduction of the tool traverse speed leads to better distribution and separation of the zirconium-silicate particles in the ground phase, which increases the pinning effect of reinforcing particles and causes grain refinement. At lower traverse speeds, due to higher inlet heat, the annealing effect is more significant. At higher traverse speeds, the dynamic recrystallization overcomes other factors, due to the more intense particle dispersion, and the grain size reduces. However, as the tool traverse speed gets larger values, the annealing effect overcomes other factors, such as dynamic recrystallization, which increases the average particle size in the SZ. An optimum traverse speed of 20 mm/min is obtained in this study.

The effect of the pass number on microhardness behavior has also been studied. Figure 10c shows the SZ microstructure of the AL6061-T6/ZrSiO₄ composite with 1, 2, and 4 passes at $V_{RS} = 1000$ rpm and $V_{TS} = 20$ mm/min. As depicted in Figure 10c, the microhardness of the composite has increased by increasing the number of passes. Plastic deformation intensifies the dynamic

recrystallization phenomenon and causes grain refinement as the pass number increases. The formation of different intermetallic phases, the better distribution of zirconium-silicate particles, and grain boundary resistance have reduced the grain size and increased the microhardness. It should be noted that with increasing the number of passes, the average grain size decreases rapidly at first, and then the speed of this process decreases.

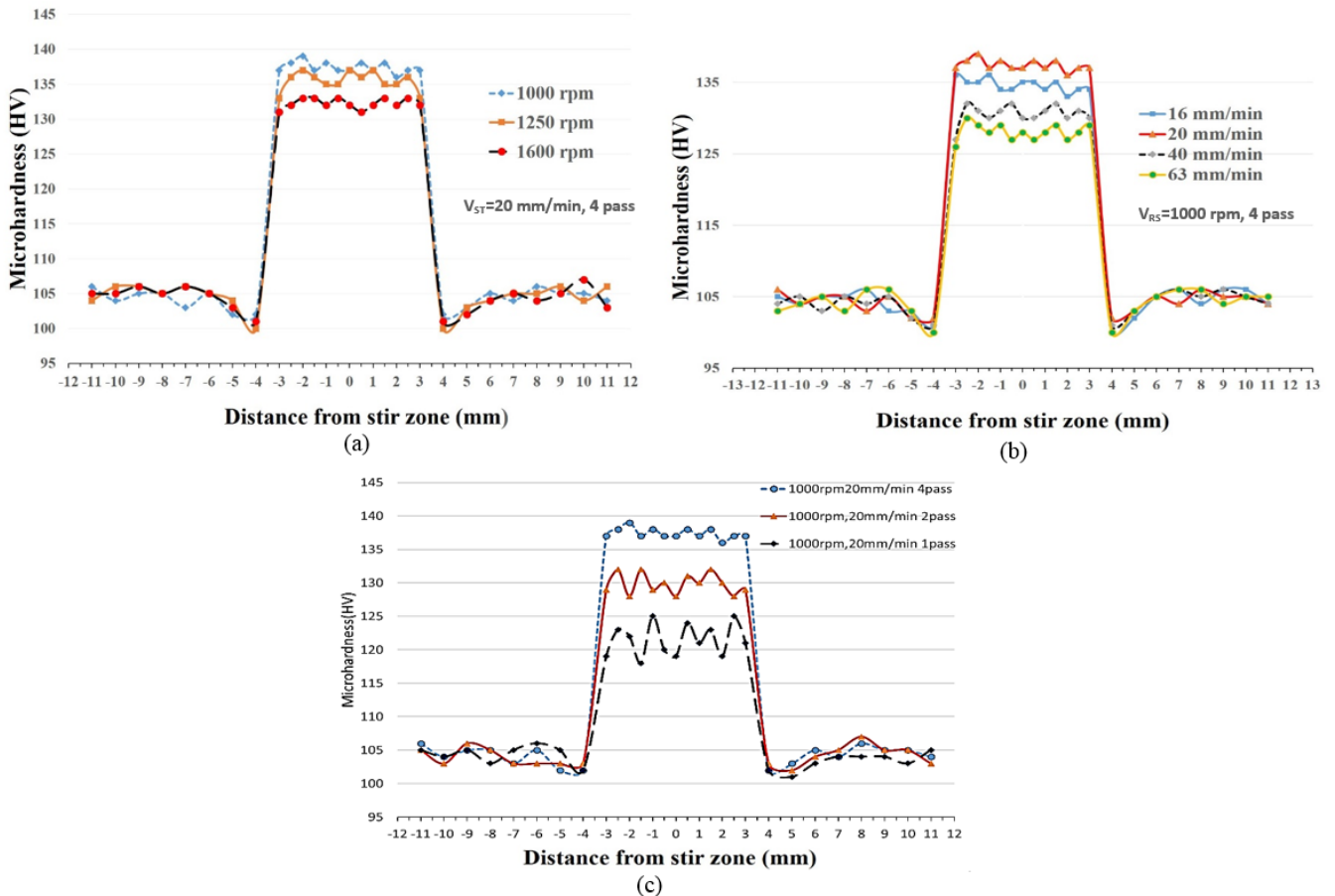


Figure 10. Microhardness of the AL6061-T6/ZrSiO₄ composite with a) different tool rotational speeds, b) different tool traversing speeds, and c) different pass numbers

Significant changes in the strength behavior of the FSPed samples are observed in the AL6061-T6/ZrSiO₄ composite. The size of the grains is reduced, elongation is decreased and a brittle failure is obtained during the tensile tests. In all investigated specimens, fracture occurred due to the crack propagation, and no choking was observed. It indicates the presence of continuous points for crack nucleation and propagation. These points can be porosities in the composites or possible points of the ZrSiO₄ particle accumulation.

First, the effect of tool rotational and traverse speeds on the tensile strength is investigated. Figure 11a shows the stress-strain curve of the composite produced with four passes, $V_{TS} = 20$ mm/min, and different rotational speeds of $V_{RS} = 800, 1000, 1250,$ and 1600 rpm. It can be seen that the ultimate strength of the base metal has increased in all samples. The ultimate strength of the FSPed aluminum composite, reinforced with zirconium-silicate particles, is higher than unprocessed aluminum in all cases. However, by increasing the rotational speed, the annealing effect overcomes other factors and

increases the particle size of the composite. Therefore, with increasing grain size, the ultimate tensile strength (UTS) decreases according to the Hall-Patch relationship. Hence, the ultimate tensile strength at $V_{RS} = 1600$ rpm has the lowest value. Among the selected rotational speeds, $V_{RS} = 1000$ rpm has recorded the highest tensile strength compared to other cases.

Figure 11b shows the stress-strain curves of the FSPed composites with four passes $V_{RS} = 1000$ rpm and different traverse speeds, i.e. $V_{TS} = 16, 20, 40,$ and 63 mm/min. As the tool progresses faster, the ultimate tensile strength of the specimens decreases. The reduction of tool traverse speed leads to the better distribution and separation of zirconium-silicate particles in the base metal and intensifies the pinning effects. Therefore, the grain size is reduced. At lower traverse speeds, the annealing effect is more significant, due to higher inlet heat. However, the pinning effect dominates other factors, because of more intense particle dispersion. Hence, dynamic recrystallization leads to the grain refinement. The effect of the pass number on the tensile strength is illustrated in Figure 11c. Constant traverse and rotational speeds of $V_{TS} = 20$ mm/min and $V_{RS} = 1000$ rpm are chosen and the pass number is varied from one to four. It can be seen that by applying the FSP process in different passes, the yield stress of the SZ generally increases. An increase in the number of FSP passes increases the temperature and strengthens the bonds between the base phase and the reinforcing particles. Due to the homogeneous and uniform distribution of the reinforcing particles, the volumes of the dislocations and porosities are reduced. Hence, the pinning effect increases and the accumulation of the zirconium-silicate particles reduces. Therefore, the possibility of failure decreases. Using four passes was ideal in the FSP process of AL6061-T6/ZrSiO4 composites.

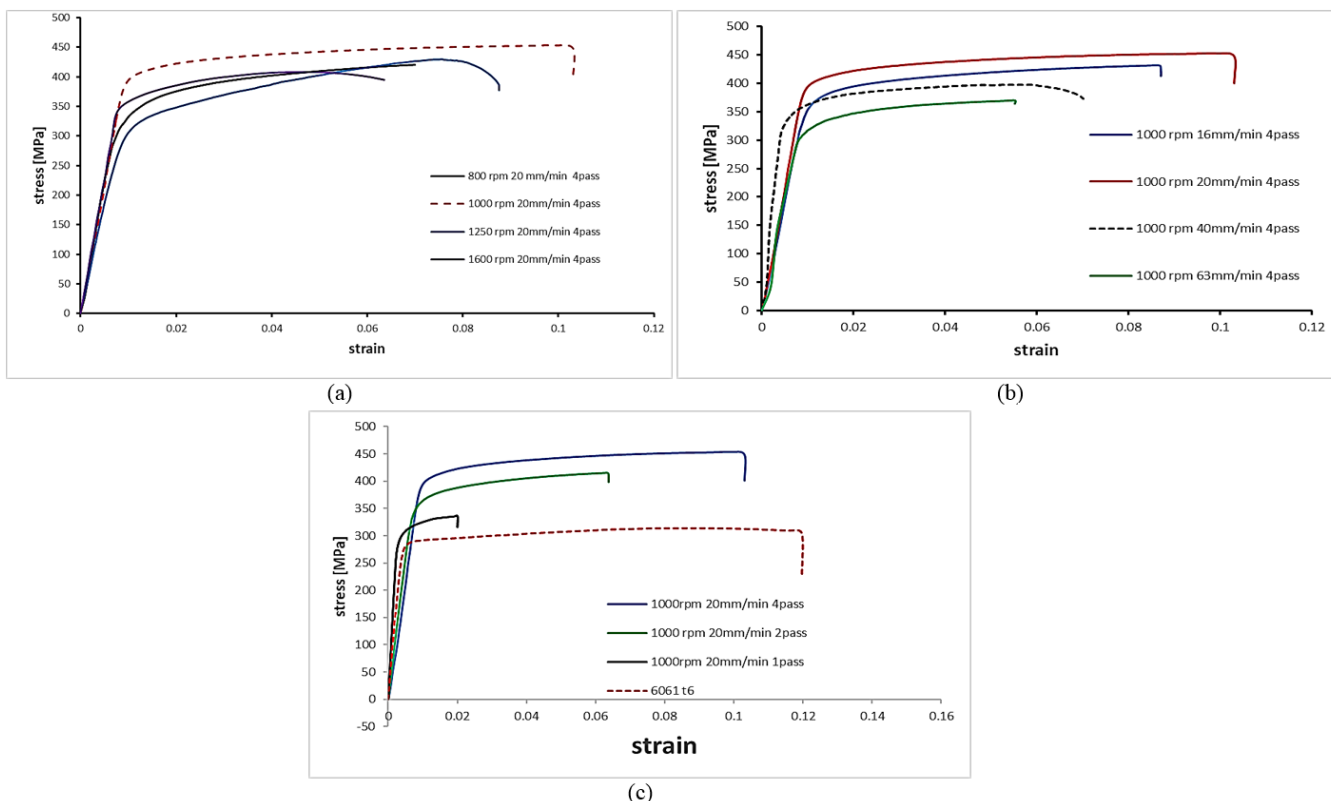


Figure 11. Stress-strain curves of the AL6061-T6/ZrSiO4 composite with a) different tool rotational speeds, b) different tool traverse speeds, and c) different pass numbers

Table 2 shows comparisons of previous studies carried out on FSP applications for the fabrication of aluminum metal matrix surface composites. The results of the present study are compared with those of references [9,23,41,43]. The table shows the values of the ultimate strength and hardness of FSPed surface composites with aluminum as the base metal and different reinforcing particles. The strength and hardness of the AL6061-T6/ZrSiO₄ composites produced in this study are significantly larger than those of other studies. The FSP reinforcing of AL6061-T6 with ZrSiO₄ particles in the present investigation gives rise to increasing the strength and hardness more efficiently than using SiO₂ and graphite [9]. According to the present study, such an order of enhancement of mechanical properties is obtained by using 5 µm ZrSiO₄ particles in AL6061-T6 alloy.

Table 2. Comparisons of various studies performed on surface composite fabrication of aluminum alloys using FSP

Base metal	Reinforcement	V _{TS} (rpm)	UTS (MPa)	Hardness HV	Ref.
AL6061-T6	ZrSiO ₄	1000	470	137	Present
AA5052	ZrSiO ₄	1000	236	97.5	[41]
AA6082	Y ₂ O ₃ +Gr	1200	300	130	[43]
AL pure	TiO ₂	1200	145	--	[23]
AL6061-T6	SiO ₂ +Gr	1120	186	89	[9]

4. Conclusion

In this research, the FSP process of aluminum 6061-T6 alloy was successfully performed. The effect of zirconium-silicate reinforcing particles on the microstructure and mechanical properties of the AL6061-T6/ZrSiO₄ composite, including microhardness and tensile properties, was investigated. Excellent dispersion of ZrSiO₄ particles in the aluminum matrix is observed in the SEM micrographs of the fractured surface of the tensile test specimen. This indicated that the composite material is homogenous and the composite fabrication was successful. The obtained results are as follows:

- Microscopic examination of the FSPed region and the base metal by optical microscope has shown that the average grain size in the stirred zone is smaller than the base metal. Therefore, the fabricated composite had a more homogeneous structure and less porosity.
- The zirconium-silicate reinforcing particles have filled the small pores in the base metal and thus increased the hardness.
- The use of zirconium-silicate reinforcing particles increased the mechanical crystallization and resulted in grain refinement in the SZ. Thus, it increased the tensile strength.
- The 1000 rpm rotational speed had better mechanical properties than other speeds.
- The use of 20 mm/min traverse speed increased the mechanical properties compared to other cases, which was attributed to increasing the dynamic recrystallization, pinning effects, and good distribution of ZrSiO₄ particles in the base metal.
- Increasing the pass number caused a more homogeneous microstructure and a better distribution of reinforcing particles and hence increased the strength of the stirred zone. The yield strength of the base metal increased from about 290 MPa to 430 MPa using the FSP process of AL6061-T6 reinforced with ZrSiO₄ particles.

5. References

- [1] Mironov, S., Sato, Y.S. and Kokawa, H. 2019. Nanocrystalline Titanium, Chapter 4 - Friction-stir processing. Elsevier. doi:10.1016/B978-0-12-814599-9.00004-3.
- [2] Kwon, Y.J., Shigematsu, I. and Saito, N. 2003. Mechanical Properties of Fine-Grained Aluminum Alloy Produced by Friction Stir Process. Scripta Material. 49:785-789. doi:10.1016/s1359-6462(03)00407-x.
- [3] Nakata, K., Kim, Y.G., Fujii H., Tsumura, T. and Komazaki, T. 2006. Improvement of mechanical properties of aluminum die casting alloy by multi-pass friction stir processing. Material Science and Engineering A. 437:274-280. doi:10.1016/j.msea.2006.07.150.
- [4] Su, J.Q., Nelson, T.W. and Sterling, J.C. 2006. Grain refinement of aluminum alloys by friction stir processing. Philosophical Magazine. 86:1-24. doi:10.1080/14786430500267745.
- [5] Elangovan, K., Balasubramanian, V. and Valliappan, M. 2008. Effect of tool pin profile and tool rotational speed on mechanical properties of friction stir welded AA6061 aluminium alloy. Materials and Manufacturing Processes. 23:251-260. doi:10.1080/10426910701860723.
- [6] Karthikeyan, L., Senthikumar, V.S., Balasubramanian, V. and Natarajan, S. 2009. Mechanical property and microstructural changes during friction stir processing of cast aluminum 2285 alloy. Materials and Design. 30:2237-2242. doi:10.1016/j.matdes.2008.09.006.
- [7] Morishige, T., Tomotake, H., Tsujikawa, M. and Higashi, K. 2010. Comprehensive analysis of minimum grain size in pure aluminum using friction stir processing. Material Letter. 64:1189-1200. doi:10.1016/j.matlet.2010.06.003.
- [8] Al-Fadhalah, K.J., Almazrouee, A.I. and Aloraier, A.S. 2013. Microstructure and mechanical properties of multi-pass friction stir processed aluminum alloy 6063. Materials and Design. 53:550-560. doi:10.1016/j.matdes.2013.07.062.
- [9] Devaraju, A., Kumar, A. and Kotiveerachari, B. 2013. Influence of rotational speed and reinforcements on wear and mechanical properties of aluminum hybrid composites via friction stir processing. Materials and Design. 45:576-585. doi:10.1016/j.matdes.2012.09.036.
- [10] El-Rayes, M.M. and El-Danaf, E.A. 2012. The influence of multi-pass friction stir processing on the microstructural and mechanical properties of aluminum alloy 6082. Journal of Materials Processing Technology. 212:1157-1168. doi:10.1016/j.jmatprotec.2011.12.017.
- [11] Rasouli, S., Behnagh, R.A., Dadvand, A. and Saleki-Haselghoubi, N. 2016. Improvement in corrosion resistance of 5083 aluminum alloy via friction stir processing. Proceeding of Institute of Mechanical Engineering Part. L. Journal of Materials: Design and Application. 230:142-150. doi:10.1177/1464420714552539.
- [12] Alishavandi, M., Ebadi, M. and Kokabi, M.H. 2021. Optimization of parameters for the friction stir processing and welding of AA1050 aluminum alloy. Iranian Journal of Materials Science and Engineering. 18:1-11. doi:10.22068/ijmse.2016.
- [13] Valeeva, A.K., Akhunova, A.K., Imayev, M.F. and Fazlyakhmetov, R.F. 2020. Effect of friction stir processing on the strengthening of the 2024 aluminum alloy. IOP Conf. Series: Materials Science and Engineering. 1008:012025. doi:10.1088/1757-899X/1008/1/012025.
- [14] Mirian Mehrian, S.S., Rahsepar, M., Khodabakhshi, F. and Gerlich, A.P. 2021. Effects of friction stir processing on the microstructure, mechanical and corrosion behaviors of an aluminum-

- magnesium alloy. *Surface and Coatings Technology*. 405:126647. doi:10.1016/j.surfcoat.2020.126647.
- [15] Karimi, M., Asefnejad, A., Aflaki, D., Surendar, A., Baharifar, H., Saber-Samandari, S., Khandan, A., Khan, A. and Toghraie, D. 2021. Fabrication of shapeless scaffolds reinforced with baghdadite-magnetite nanoparticles using a 3D printer and freeze-drying technique. *Journal of Materials Research and Technology*. 14:3070-3079. doi:10.1016/j.jmrt.2021.08.084.
- [16] Liang, H., Sadat Mirinejad, M., Asefnejad, A., Baharifar, H., Li, X., Saber-Samandari, S., Toghraie, D. and Khandan, A. 2022. Fabrication of tragacanthin gum-carboxymethyl chitosan bio-nanocomposite wound dressing with silver-titanium nanoparticles using freeze-drying method. *Materials Chemistry and Physics*. 279:125770. doi:10.1016/j.matchemphys.2022.125770.
- [17] Soleymani, S., Abdollah-zadeh, A. and Alidokht, S.A. 2012. Microstructural and tribological properties of Al5083 based surface hybrid composite produced by friction stir processing. *Wear*. 278–279:41–47. doi:10.1016/j.wear.2012.01.009.
- [18] Arun Kumar, R., Aakash Kumar, R.G., Ahamed, K.A., Alstyn, B.D. and Vignesh, V. 2019. Review of friction stir processing of aluminium alloys. *Materials Today*. 16:1048–1054. doi:10.1016/j.matpr.2019.05.194.
- [19] Moustafa, E.B., Abushanab, W.S., Melaibari, A., Mikhaylovskaya, A.V., Abdel-Wahab, M.S. and Mosleh, A.O. 2021. Nano-surface composite coating reinforced by Ta₂C, Al₂O₃ and MWCNTs nanoparticles for aluminum base via FSP. *Coatings*. 11:1496. doi:10.3390/coatings11121496.
- [20] Liu, Y., Chen, G., Zhang, H., Yang, C., and Shi, Q. 2012. In situ exfoliation of graphite for fabrication of graphene/aluminum composites by friction stir processing. *Materials Letters*: 301: 130280. doi:10.1016/j.matlet.2021.130280.
- [21] Huang, G., Hou, W. and Shen, Y. 2018. Evaluation of the microstructure and mechanical properties of WC particle reinforced aluminum matrix composites fabricated by friction stir processing. *Mater Charact*. 138:26-37. doi:10.1016/j.matchar.2018.01.053.
- [22] Balakrishnan, M., Dinaharan, I., Palanivel, R. and Sathiskumar, R. 2019. Effect of friction stir processing on microstructure and tensile behavior of AA6061/Al₃Fe cast aluminum matrix composites. *Journal of Alloys and Compounds*. 785:531-541. doi:10.1016/j.jallcom.2019.01.211.
- [23] Madhu, H.C., Ajay Kumar, P. and Perugu, C.S. 2018. Microstructure and mechanical properties of friction stir process derived Al-TiO₂ nanocomposite. *Journal of Materials Engineering and Performance*. 27:1318-1326. doi:10.1007/s11665-018-3188-y.
- [24] Bauri, R., Yadav, D. 2018. *Metal Matrix Composites by Friction Stir Processing*. Elsevier. doi:10.1016/B978-0-12-813729-1.00005-X.
- [25] Asadi, P., Faraji, G. and Besharati, M.K. 2010. Producing of AZ91/SiC composite by friction stir processing (FSP). *International Journal of Advanced Manufacturing and Technology*. 51:247–260. doi:10.1007/s00170-010-2600-z.
- [26] Dolatkhan, A., Golbabaie, P., Besharati Givi, M.K. and Molaiekiya, F. 2012. Investigating effects of process parameters on microstructural and mechanical properties of Al5052/SiC metal matrix composite fabricated via friction stir processing. *Materials and Design*. 37:458–464. doi:10.1016/j.matdes.2011.09.035.

- [27] Zuhailawati, H., Halmy, M.N., Almanar, I.P. and Dhindaw, B.K. 2014. Friction stir processed of 6061-T6 aluminum alloy reinforced with silica from rice husk ash. *Advanced Materials Research*. 1024:227–230. doi:10.4028/www.scientific.net/amr.1024.227.
- [28] Sharma, H., Kumar Tiwari, S., Singh Chauhan, V., Kumar, R. and Gulati, P. 2021. Wear analysis of friction stir processed aluminum composite reinforced by boron carbide. *Materials Today*. 46:2141–2145. doi:10.1016/j.matpr.2021.02.468.
- [29] Khethier Abbass, M. and Baheer, N.A. 2020. Effect of SiC particles on microstructure and wear behavior of AA6061-T6 aluminum alloy surface composite fabricated by friction stir processing. *IOP Conf. Series: Materials Science and Engineering*. 671: 012159. doi:10.1088/1757-899X/671/1/012159.
- [30] Dwivedi, P., Sachin Maheshwari, S. and Siddiquee, A.N. 2022. Investigation on aluminum based surface composite through FSP using metal (Fe-Sn-Mn) and ceramic (SiC) reinforcements. *Materials Today*. 62:251–254. doi:10.1016/j.matpr.2022.03.222.
- [31] Subramani, N., Haridass, R., Krishnan, R., Manikandan, N. and Baskaran, A. 2021. Fabrication of hybrid (AA6061/SiCp/B4C) composites using FSP method and analysing the thermal behaviour in the weld region. *Materials Today*. 47:4306–4311. doi:10.1016/j.matpr.2021.04.601
- [32] Ande, R., Gulati, P., Kumar Shukla, D. and Dhingra, H. 2019. Microstructural and wear characteristics of friction stir processed Al-7075/SiC reinforced aluminum composite. *Materials Today*. 18:4092–4101. doi:10.1016/j.matpr.2019.07.353.
- [33] Gopi, K. R., Mohandas, K. N., Reddappa, H. N. and Ramesh, M. R. 2013. Characterisation of as cast and heat treated aluminium 6061/Zircon sand/graphite particulate hybrid composites. *International Journal of Engineering and Technology*. 5:340-344. doi:10.13140/RG.2.2.36677.24803.
- [34] Rino, J.J., Sivalingappa, D., Koti, H. and Jebin, V.D. 2013. Properties of Al6063 MMC reinforced with zircon sand and alumina. *Journal of Mechanical and Civil Engineering*. 5(5):72-77.
- [35] Raju H.T. and Ramamurthy, V.S. 2018. Fabrication and evaluation of properties of aluminum alloy zirconium silicate particles reinforced metal matrix composites: A review. *International Journal of Innovative Research in Science, Engineering and Technology*. 7(11): 9284-9288. doi:10.15680/IJRSET.2018.0711021.
- [36] Thandallam, S.K., Ramanathan, S. and Sundarrajan S. 2015. Synthesis, microstructural and mechanical properties of ex situ Zircon particles (ZrSiO₄) reinforced metal matrix composites (MMCs): A review. *Journal of Research Materials and Technology*. 4(3):333-347. <http://doi.org/10.1016/j.jmrt.2015.03.003>.
- [37] Kumar, S.T., Raghu, R., Kumar, K.K., Shalini, S. and Subramanian, R. 2018. Optimisation of three body abrasive wear behavior of stir cast A356/ZrSiO₄ metal matrix composite. *Tribology in Industry*. 40(4):633-642. doi:10.24874/ti.2018.40.04.10.
- [38] Ramnath, B.V., Elanchezian, C., Naveen, E., Nagarajkrishnan, P., Chezhian, T., Saleem, A. and Srivalsan, M. 2018. Mechanical and wear behaviour of aluminum Zircon sand flyash metal matrix composite, *Proceedings of the 3rd International Conference on Materials and Manufacturing Engineering*. 390:1-8. doi:10.1088/1757-899X/390/1/012018.

- [39] Fabrizi, A., Capuzzi, S., De Mori, A. and Timelli, G. 2018. Effect of T6 heat treatment on the microstructure and hardness of secondary AlSi9Cu3(Fe) alloys produced by semi-solid. *SEED Processing Metals*. 750:1-8. doi:10.3390/met8100750.
- [40] Dhuruva Maharishi, M., Arul Marcel Moshi, A., Hariharasakthisudhan, P. and Surya Rajan, B. 2022. Investigation on the mechanical behaviour of aluminium alloy 356-Zirconium silicate metal matrix composites (AA356-ZrSiO₄ MMCs). *Silicon*. 14:11731–11739. doi:10.1007/s12633-022-01896-0.
- [41] Rahsepar, M. and Jarahimoghadam, H. 2016. The influence of multipass friction stir processing on the corrosion behavior and mechanical properties of zircon-reinforced Al metal matrix composites. *Materials Science & Engineering A*. 671:214–220. doi:10.1016/j.msea.2016.05.056
- [42] Węglowski, M.S. 2014. Friction stir processing technology–new opportunities. *Welding International*. 28:583–592. doi:10.1080/09507116.2012.753216.
- [43] Satish Kumar, T. and Shalini, Krishna Kumar, K. 2020. Effect of friction stir processing and hybrid reinforcement on wear behaviour of AA6082 alloy composite. *Materials Research Express*. 7: 026507. doi:10.1088/2053-1591/ab6e2a.